Electric Vehicle Aggregator as an Automatic Reserves Provider under Uncertain Balancing Energy Procurement

I. Pavić, *Member*, *IEEE*, H. Pandžić, *Senior Member*, *IEEE* and T. Capuder, *Member*, *IEEE*

***Abstract*—Shift of the power system generation from the fossil to the variable renewables prompted the system operators to search for new sources of flexibility, i.e., new reserve providers. With the introduction of electric vehicles, smart charging emerged as one of the promising solutions. However, electric vehicle aggregators face the uncertainty both on the reserve activation and the electric vehicle availability. These uncertainties can have a detrimental effect on both the aggregators' profitability and users' comfort.**

State-of-the art literature mostly neglects the reserve activation or it's uncertainty. On top of that, they rarely model European markets which are different that those commonly addressed in the literature. This paper introduces a new method for modeling the reserve activation uncertainty, also termed as balancing energy procurement in the European context, based on the real historic data from the European power system. Three electric vehicle scheduling models were designed and tested: the deterministic, the stochastic and the robust. The results demonstrate that the current deterministic approaches inaccurately represent the activation uncertainty and that the proposed models that consider uncertainty, both the stochastic and the robust, substantially improve the results. Additionally, the sensitivity analysis for the robust model was performed and it demonstrates how a decision-maker can choose its level of conservativeness, portraying its risk-awareness.

***Index Terms*—Electric Vehicles, Electric Vehicle Aggregator, Frequency Containment Reserve, Frequency Restoration Reserve, Uncertainty**

I. Nomenclature and Abbreviations

A. Nomenclature

1) Sets and Indices:

$\mathcal{S}$	Set of scenarios, indexed by $s \in \{1, N_s\}$,
$\mathcal{T}$	Set of timesteps, indexed by $t \in \{1, N_t\}$,
$\mathcal{V}$	Set of vehicles, indexed by $v \in \{1, N_v\}$.

2) Input Parameters:

Δ	Duration of a timestep [h],
Λ	Maximum duration of the RA,
$A^{\{\text{UP/DN}\}\_\{\text{FCR/aFRR}\}}$	Fixed up/down FCR/aFRR RA ratio,
C_v^{B}	Capital battery cost for EV v [€],
$C_{v,t}^{\text{FCH}}$	Fast charging fee [€/kWh],
C_t^{DA}	Day-ahead market electricity price [€/kWh],
B_v	Battery capacity of EV v [kWh],
$CA_t^{\{\text{UP/DN}\}\_\{\text{FCR/aFRR}\}}$	Reserve activation fee [€/kWh],
$CR_t^{\{\text{UP/DN}\}\_\{\text{FCR/aFRR}\}}$	Reserve capacity fee [€/kW/Δ],
$D_{\{1/2/3/4\}}^{\text{B}}$	Battery degradation coefficients,
$E_{v,t}^{\text{RUN}}$	Energy used for driving of EV v [kWh],
$P_{v,t}^{\text{CP\_MAX}}$	Charging point maximum power limit [kW],
$P^{\text{FCH\_MAX}}$	Maximum power limit for fast charging [kW],
$P_v^{\text{OBC\_MAX}}$	Max. on-board-charger power for EV v [kW],
$SOE_v^{\{\text{MIN/MAX}\}}$	Minimum/maximum SOE of EV v [%],
SOE_v^{T0}	Initial SOE of EV v [%],
$\eta^{\{\text{RUN/V2G}\}}$	EV driving/V2G discharging efficiency,
$\eta^{\{\text{FCH/SCH}\}}$	EV fast/slow charging efficiency.

3) Variables:

c^{OTH}	Aggregator costs other than reserve activation [€],
c^{ACT}	Aggregator costs arising from reserve activation [€],
$c_{v,t}^{\text{DEG}}$	Degradation cost attributed to EV v [€],
$e_{v,t}^{\{\text{BUY/SELL}\}\_\text{DA}}$	Energy traded in the DA market [kWh],
$e_{v,t}^{\text{DCH}}$	Energy discharged from EV v [kWh],
$e_{v,t}^{\{\text{FCH/SCH}\}}$	Energy fast/slow-charged to EV v [kWh],
$e_{v,t}^{\text{DEG}}$	Energy used to calculate battery degradation of EV v [kWh],
$e_{v,t}^{\text{OTH}}$	Accumulated energy other than from RA [MWh],
$e_{v,t}^{\text{ACT}}$	Accumulated energy from RA [MWh],
$r_{v,t}^{\{\text{UP/DN}\}\_\{\text{FCR/aFRR}\}}$	Capacity sold in reserve markets [MW],
$soe_{v,t}^{\text{EV}}$	State-of-energy of EV v [kWh].

B. Abbreviations

ARC	Accepted Reserve Capacity,
ARE	Activated Reserve Energy,
aFRR	automatic Frequency Restoration Reserve,
CP	Charging Point,
DA	Day Ahead,
DM	Deterministic Model,
EV	Electric Vehicle,
FCR	Frequency Containment Reserve,
FRCE	Frequency Restoration Control Error,
LFC	Load Frequency Control,
mFRR	manual Frequency Restoration Reserve,
OBC	On-Board-Charger,
OF	Objective Function,
RA	Reserve Activation,
RM	Robust Model,
RUS	Robust Uncertainty Set,
RR	Replacement Reserve,
SM	Stochastic Model,
SOE	State-Of-Energy,
TSO	Transmission System Operator,
V2G	Vehicle-to-Grid (grid discharge).

This work has been supported in part by the European Structural and Investment Funds under project KK.01.2.1.02.0063 SUPEER (System for optimization of energy consumption in households), as well as by the Croatian Science Foundation and European Union through the European Social Fund under project Flexibility of Converter-based Microgrids – FLEXIBASE (PZS-2019-02-7747).

II. Introduction

Electrification of the transport sector is underway and electric vehicles (EVs) are rapidly increasing their market share [1]. Large EV fleets can have an adverse effect on the overall power system if inadequately controlled, e.g. increasing the peak power and the balancing needs. The conventional power system operation is already affected by the heavy penetration of renewable energy sources and decommissioning of fossil power plants. Thus, new flexibility sources are needed to effectively balance the system. Smart EV charging [2] seems to be a promising solution due to the EVs' high storage capability [3] and availability during the day [4].

A. Balancing Services and Markets

Balancing the European power system is based on four types of reserves [5]: Frequency Containment (FCR), automatic (aFRR) and manual (mFRR) Frequency Restoration, and Replacement Reserve (RR). The FCR and aFRR are automatically activated reserves (activated upon a frequency deviation and an automatic generation control signal, respectively) with fast response and short but more frequent activation events. FCR is used to intervene automatically within seconds in the entire synchronous area to restore the balance between the supply and the demand [6]. It acts as a first response to frequency disturbances. A provider must be able to ramp up/down its generation/consumption to the full power within 30 seconds after a disturbance. The frequency value after a successful FCR activation is at a stable value below or above 50/60 Hz (nominal value). The task of restoring the frequency to its nominal value is performed by aFRR and mFRR. Power imbalances can cause changes in power flows between different areas and those imbalances are compensated regionally by the so-called "Load Frequency Control (LFC) areas" [5]. The TSOs in each LFC area continuously calculate deviations between the measured and the scheduled power exchange to their LFC area. Those deviations are called frequency restoration control error (FRCE) which serves as an input to a frequency restoration controller. The controller operates with a few seconds cycle and requests aFRR activation until the FRCE reaches zero or all available aFRR are fully activated. The activation time for aFRR provision is 30 seconds to 7.5 minutes (5 minutes after 2024) [7]. As the aFRR provision is gradually increasing, the FCR is released and can be used for new imbalances. The mFRR and RR are manually activated reserves (based on a signal directly sent by the TSO's dispatch center) with slower response, longer and less frequent activation events. The mFRR is manually activated to release the activated capacity of aFRR and make it available for new imbalance compensations or to provide additional frequency restoration power. Full activation time of mFRR is 12.5 minutes [7]. As the mFRR provision is gradually increasing, the aFRR is released and can be used for new imbalances. Further on, a TSO can additionally use RR to free the activated capacities in mFRR. RR is not obligatory and only few TSO use it across Europe. Full activation time of RR is 30 minutes. Similar to stationary batteries [8], EVs are technically better suited for automatic reserves [9] and providing them can yield high revenues [10]. Therefore, in this paper we exclusively focus on FCR and aFRR.

European reserve markets are organised by the TSOs and are currently independent from the short-term energy markets which are organised by the electricity exchange operators such as EPEX in Central Europe [11]. Thus, cooptimization of the reserve and energy procurement is not possible. Market participants do not submit their technical constraints toward either the TSO (for reserve market) nor the exchange operator (for energy market) but their price-quantity bids. In general, reserve markets are organised in a two-stage fashion, first being the reservation of the balancing capacity and second for activation of the balancing energy. In rest of the paper we use terms such as reserve activation or balancing energy activation/procurement interchangeably. In practice, the FCR reserve does not have a subsequent balancing energy market but only the balancing capacity market. Balancing energy is activated proportionally among all accepted bids. For other reserve types (aFRR, mFRR and RR), the participants who are cleared in the balancing capacity stage must submit their offers in the balancing energy stage at a desired price.

All reserves types in Europe have two directions: up/positive and down/negative. They can be procured symmetrically (both directions with one bid) or asymmetrically (two separate markets for each direction). The latest European regulation states that the FCR is procured symmetrically, while all other reserves must have separate markets for each direction.

Commonly, the gate closures of different markets are the following: 08:00 day-ahead for balancing capacity [13], 12:00 day-ahead for DA energy auction and less than 1 hour ahead for balancing energy. To accurately bid in the first market and mitigate the lost opportunity costs, market participants must take into account all the subsequent markets and prices. Additionally, to bid in the balancing capacity market, it is essential to estimate the volume of the potential balancing energy provision as it affects the revenue of a market participant or can create technical issues, especially for an energy-constrained technology such as batteries. Thus, the EV aggregator in this paper bids for the balancing capacity in the DA timeframe, but takes into account both the DA energy market and close-to-real-time balancing energy market. The DA market is considered to mitigate the lost opportunity costs [12] and to prepare the EV batteries for reserve provision (charge or discharge). The balancing energy market is considered to adequately calculate the benefits of the balancing capacity provision and to enable operational feasibility upon the balancing energy activation.

The model presented in this paper is well-suited for European markets, but cannot be directly applied to North-American markets. The reserves in North America can be, in general, divided into three main types: regulation, operating reserve – spinning, and operating reserve – non-spinning [14]. The regulation is used to continuously balance small deviations between the supply and the demand in the real-time following the automatic generation control signal. The units must be able to change their output in a timescale of a few seconds. It is comparable to aFRR balancing capacity in Europe. There is also, in some markets, a product called regulation mileage,

which compensates units for their performance in response to the regulation signals. This can roughly be considered as the aFRR balancing energy in Europe. The spinning operating reserve is designed to help the system during larger contingencies, and the units providing it must be online and able to ramp up within 10 to 15 minutes. This service is comparable to mFRR in Europe. The last one is the non-spinning operating reserve, designed to recover the system after large unplanned contingencies. The units providing it can be offline but must be able to ramp up to full power in 10 to 30 minutes, depending on the market.

In North America there is no market for primary frequency response (counterpart of the European FCR) as this isa mandatory service [15]. Commonly, all larger centralised power plants must withhold a certain capacity, called headroom, to be able to provide frequency response. Even though there is no market and therefore no data, one could still model the primary response uncertainty, but not for the purpose of bidding in the primary frequency response market (if such would exist) or the DA energy market, but to better prepare its technical units for its activation. However, this applies only for energy-constrained units, such as batteries, which are not obliged to provide frequency response.

In North America the independent system operators or regional transmission operators are in charge for both the energy and reserve trading. If the same operator runs both markets there are less barriers to create a co-optimized or joint auctions for all the required services. There is a high diversity between market concepts in the North America, but in general they all have some form of cooptimisation between the energy, the regulation and the reserves [14]. Once again, for the purpose of this paper the regulation (aFRR counterpart) is the only relevant reserve, while the spinning and non-spinning reserves are not considered as services interesting to EV aggregators. Contrary to European bids, which involve free price quantity bids/curves, in the North American markets each technical unit must enter its technical parameters (minimum power output, ramping limits etc.) as well as the economic part, such as the minimum generation, start-up, incremental and lost-opportunity cost [17]. The participants do not need a bidding algorithm to self-optimise and bid in separate markets. Having in mind these differences toward the European markets, the DA bidding algorithm presented in this paper is not directly applicable to the North American markets. Thus, the paper further on focuses exclusively on the European-style markets.

B. Sources of Uncertainty

Three sources of uncertainty can be linked to the EV energy and reserve provision algorithms: EVs' driving patterns, market prices and reserve activations (RA). Uncertainty on the EV behaviour negatively affects the EVs' availability to deliver the planned services and to respect the EV batteries' state-of-energy (SOE). This is usually modelled using behavior scenarios [18], [19], [20], [21] and often includes the second stage for performing re-dispatching measures [22], [23], [24], [25]. The second uncertainty stream are price uncertainties that are commonly addressed through price-taker models using price scenarios [18], [20], [21], [19] or robust models where prices are determined as a worst-case scenario for the market participant [28], [29]. Another approach are the price-maker models where the aggregated EV battery capacity is assumed to be large and the market price evolves within the model itself. In such models the participants are paid on the pay-as-bid basis [24], [26] or by the market clearing price [27].

The EV behavior and price uncertainties are, in general, well elaborated in the recent literature. However, there is a gap in the literature in addressing the RA uncertainty. Deterministic modeling of RA [22], [25], [29], [30] can create problems to EV users as well as to their aggregators [31]. The EV users may suffer from a lower SOE than required for their next trip if the activated up reserve volume was higher than anticipated. An insufficient SOE translates into a decreased comfort level for the EV users and affects their willingness to participate in reserve provision [19]. On the other hand, if the EV drivers' needs are prioritized, the aggregators may suffer from insufficient energy volumes to back up their day-ahead (DA) plans. Aggregators may experience issues in the opposite direction as well. If down reserve is more frequently activated, the EVs' SOE will be higher than expected and they will not be able to follow their DA schedule. Inability to adhere to the agreed DA schedule causes additional balancing costs [5], whereas the inability to activate the scheduled reserve leads to penalization [25], [30], [32] and eventually disqualification from the reserve market participation [24]. RA uncertainty modeling is thus essential for adequate reserve market participation. One of the possible approaches is stochastic modeling of the RA, as pursued in [18], [19], [21], [32]. However, the randomly generated RA scenarios, instead of the ones based on actual operation data, may not appropriately address the RA uncertainty [18], [19], [32]. On the other hand, employment of publicly available data such as automatic generation control signals (North American-style market [21]) or RA data from the European platforms (e.g. ENTSO-E [26]) as scenarios is more appropriate. Following this logic, the stochastic formulation in this paper is designed to utilize such data.

Robust formulation of uncertainty is another approach rarely used when considering the RA and, to the best of the authors knowledge, only one paper [29] pursues this idea. It considers RA as two values: the number of RA during the day (an integer value) accompanied with a binary value for each call indicating whether the reserve is fully activated or not activated at all. However, such modelling approach is more adequate for manual reserves, while automatic reserves require a more rigorous approach. Following this approach, our paper robustly designs the RA uncertainty of the automatic reserves.

C. Contributions and Paper Organisation

We model two types of reserves (FCR and aFRR) simultaneously and perform a comparison between their scheduling. Contrary to the majority of papers that tackle only the North American-style markets, we focus on modeling the uncertainty of automatic RA for an EV aggregator based on real data stemming from the European-style markets. Although European markets were already investigated in [24], [25], [26], none

of these modeled two types of automatic reserves and none of these based the uncertainty modeling on publicly available RA data. This paper, for the first time, models and compares the RA uncertainty using the stochastic and the robust approach.

In this paper we model a price-taker EV aggregator with the assumption of perfect forecasts of energy, balancing capacity and balancing energy prices. The effect of the price forecasts errors can be easily integrated in the model as discussed extensively in the literature, e.g. [18], [20], [21], [19], [28], [29]. Additionally, price uncertainty correlated with tradable volumes, as in the case of balancing energy whose prices can rise significantly when the system is highly imbalanced, can be modeled using the aggregated price curves. The same curve can be used to model the price-maker approach as well [27]. The reason why we did not model this uncertainty is because the focus of this paper are the effects and means to model the reserve activation uncertainty, not the price uncertainty.

Each EV in this paper is modeled individually using its own variables, parameters and constraints assuring that each EV is able to fulfill the scheduled reserves. It means that the worst-case scenario with robust formulation is applied to each EV individually, not only at the fleet level.

Thus, we summarize contribution of the paper as follows:

1) it statistically analyses the aFRR and FCR historical data to define the set of RA scenarios as well as US for the RA,
2) it integrates a newly created scenario set and US of aFRR and FCR RA into an EV model and casts it as a stochastic or a robust linear program,
3) it designs a data-driven robust optimization model for reserve and energy bidding of an EV fleet model with RA as the source of uncertainty,
4) it builds an EV aggregator model for reserve and energy bidding, where individual EV constraints are modeled finding the worst-case RA for each EV in the fleet,
5) it simulates a simultaneous provision of aFRR, FCR and DA energy and proves the efficiency and adequacy of the designed models as compared to the deterministic model.

The rest of the paper is organized as follows. Section III provides statistical analyses of RA and determines the input parameters for RA modeling for all observed approaches. The mathematical background is formulated and elaborated in Section IV, while the input parameters are elaborated and case studies are defined in Section V. The simulation results are presented in Section VI, while Section VII highlights the most important findings and concludes the paper.

III. Defining RA Uncertainty

We design three models to adequately address the RA: the deterministic model (DM), the stochastic model (SM) and the robust model (RM). They all require some kind of input parameters for the RA modeling. A statistical analysis of the RA behavior is required to gain those inputs.

A. Statistical Analysis

The main analyzed parameter is the RA ratio, which is defined as the ratio of the Activated Reserve Energies (ARE) and Accepted Reserve Capacity (ARC) both for FCR and aFRR. The bids are taken from the RTE (French TSO) for the year 2018 [35].

The RTE data is published in 30-minute resolution as this is the imbalance settlement period and balancing energy remuneration period in France. Currently, FCR and aFRR markets in Europe operate in 4-hours resolution, but the European trend is to lower the validity periods as much as possible. For example, the future aFRR balancing energy platform for Europe-wide trading will be based on a 15-minute time period [7]. Regardless on the timestep duration, the only important parameter for an aggregator and individual EV batteries is how much in total, during one timestep, certain reserve in certain direction is activated. In other words, the frequency dynamics within the validity period do not affect our bidding algorithm. However, to compete in the FCR of aFRR markets, any reserve provider must pass a prequalification process where the dynamics, ramping and other technical detail are tested.

For each half-hourly period (and each reserve type and direction) the RA quantities are calculated as:

$$\left(RA\_ratio_t = \frac{ARE_t}{ARC_t \cdot \Delta}\right)^{\{\text{UP/DN}\}\_\{\text{FCR/aFRR}\}} \tag{1}$$

Visualization of the obtained results from the statistical analyses for FCR and aFRR is presented in Figure 1. These data are further used to determine the scalar inputs for the DM (annual average values equal in all timesteps), to select scenarios for the SM, and to obtain bounds for the RUS. Also, this dataset will be used to select RA scenarios for the ex-post validation of the models.

Probability distribution functions for up (UP) and down (DN) reserves are very similar for both the FCR and the aFRR, as shown in Figure 1. The down reserve has a slightly higher annual average for both the FCR and the aFRR. Also, average values for both UP and DN directions are much higher for aFRR than for FCR. These values are used in the DM as fixed inputs and are provided in the second column in Table I, under parameter A, which expresses the share of the accepted balancing capacity to be activated in the deterministic setup.

Scenarios for the SM are taken as the realized RA ratios for each reserve type and direction from Jan. 11-20, 2018 (10 in total). An ex-post validation is performed on scenarios from April 1, 2018 to July 9, 2018 (100 in total). The examples of the used scenarios are presented in Figure 2, indicating high uncertainty range. Each curve represents an RA ratio for one type of reserve and direction.

B. Robust Model Parameters

An extensive data analysis we performed indicates there is no correlation between the FCR and the aFRR RA during one timestep in one direction. However, there is a correlation between the UP and DN RA for both the FCR and aFRR.

The RA ratios for UP and DN reserves are dependent variables where a high RA value for one direction entails a low RA value for the other. This is valid for both the FCR and aFRR. This is modeled in eq. (32) in Section IV-C2 and shown as green (max) and cyan (99%) lines on the scatter

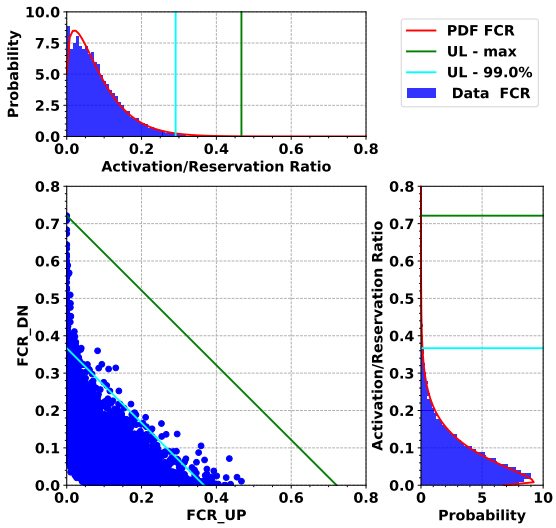

(a). Frequency containment reserve activation ratios

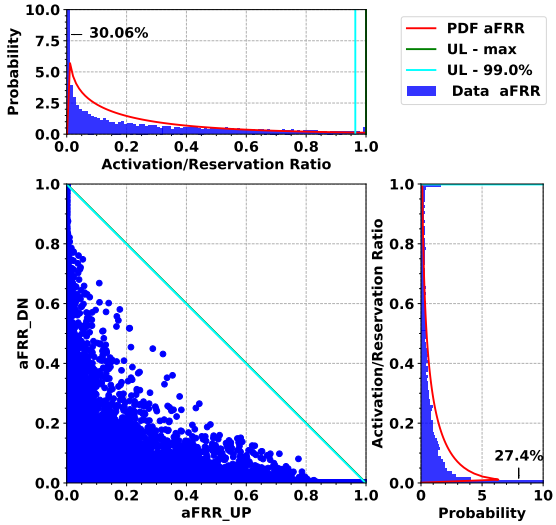

(b). Automatic frequency restoration reserve activation ratios

Fig. 1. Activation ratios – historical data (UL - Upper Limit)

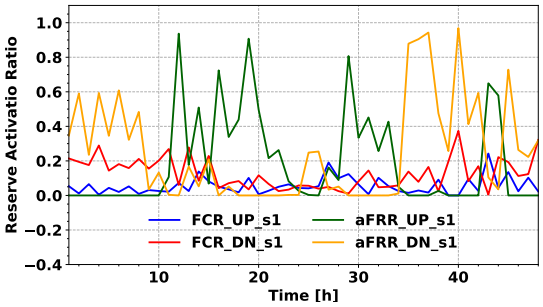

Fig. 2. Reserve activation scenario examples

graphs in Figures 1a and 1b. This means that the correlation between the two directions is considered in our RUS. The same equation/line also bounds the individual RA ratios of the UP and DN reserves. FCR UP and DN are never zero at the same time (there is always a slight imbalance in one direction). However, those values are small (less than 5% of the total balancing capacity) and therefore omitted from the mathematical model. On the contrary, aFRR UP and DN could be zero at the same time, thus the lower bound for their correlated activation is not necessary.

To properly model the RA for the DA bidding purposes we must understand the three different RA timeframes: instantaneous RA, RA during one market timestep (30 min), RA during the whole trading horizon (24 hours). Instantaneous RA refers to the power applied as a response to frequency deviation signals. Instantaneous RA means that the reserve in each moment can be activated fully (up to the accepted balancing capacity bid), partially or not activated at all. This requirement is covered with power constrains where the total charging/discharging power of each EV is limited by the available capacity. We do not impose uncertainty here, if EVs are obliged to provide a reserve they will always have sufficient power to do so.

The other two RA timeframes do not refer to power, but to energy activated during a certain period. During one timestep, the FCR and aFRR can be, theoretically, activated fully (the RA lasts for 30 min), partially (RA duration shorter than 30 min) and not activated at all. Blue dots/bars in Figure 1 represent this timeframe. The historical data provided in Figure 1a indicates that the FCR will never be fully activated during an entire market timestep (30 min), i.e. FCR RA ratio never reaches 1. The maximum ratio for FCR UP RA is 0.47 and for DN RA 0.73 (presented in Figure 1a with the green-colored line in bar graphs). In 99% of the time the FCR UP and DN RA ratios are lower or equal to 0.29 and 0.36, respectively (presented in Figure 1a with the teal-colored line in bar graphs). High aFRR RA ratios during one timestep are also rare, but more frequent than in the case of FCR. The aFRR is sometimes fully activated during the entire timestep in both directions. In 99% of the time, the aFRR UP and DN RA ratios are lower or equal to 0.96 and 1, respectively (presented in Figure 1b with the teal-colored line). The maximum RA ratios in one timestep (noted as parameter A^{MAX}) used for the RUS in the main case study are given in Table I. Those in the third column are used for the OF of the robust subproblem and those in the fifth column are used for the robust subproblems related to technical constraints containing uncertain parameters. It can be seen that the OF of the robust subproblem uses lower values for the A^{MAX} for FCR, neglecting 1% of the historically largest RA. The technical robust subproblems are more conservative and do not neglect high RA for FCR.

The third timeframe to be observed is the RA during the whole trading horizon (24 hours), referring to the summation of all half-hourly RA ratios during each day of the year. It can be visualised as a summation of all blue bars in bar graphs in Figure 1.

The daily sums of the RA ratios (i.e. specific daily balancing energy) can, theoretically, take values from zero (no activations) to 48 (full activation of a reserve at all times). Throughout the year these values are always within certain upper and lower limits represented with Υ and Γ in formulations stated in the RUS and explained in details in Section IV-C2.

Parameter Υ used in equations in Section IV-C2 states that a reserve must be either fully activated at least Υ timesteps or partially activated during more timesteps, where the summation of those partial RA is at least equal to Υ. Parameter Γ used in equations in Section IV-C2 states that a reserve must

TABLE I
RESERVE ACTIVATION INPUTS FOR DETERMINISTIC AND ROBUST MODELS

Model	DM	RM for eq. (26)		RM for eqs. (27)–(30)		
Parameter	A	A^{MAX}	$\Gamma = \Upsilon$	A^{MAX}	Υ	Γ
Input	Mean	0.99%	Med	Max	Min	Max
UP_FCR	0.082	0.36	4	0.73	0.93	8.21
DN_FCR	0.085		3.8		1.10	16.64
UP_aFRR	0.198	1	9.13	1	2.10	21.31
DN_aFRR	0.218		9.70		2.62	20.51

be either fully activated up to Γ timesteps or partially activated during more timesteps, where the summation of those partial RA is up to Γ.

Medians of the daily sums of RA for each reserve and direction are provided in Table I in column four (Med). These numbers are used as both Υ and Γ parameters for the OF of the robust subproblem. Using the same value for Υ and Γ means that this subproblem does not assume uncertainty in the total daily RA but only uncertainty related to the distribution of the RA throughout the day. The minimum and maximum of the daily sums for each reserve and direction are given in Table I in the penultimate and ultimate columns. These numbers are later used as Υ and Γ parameters for the robust subproblems related to technical constraints containing uncertain parameters. Using different values for Υ and Γ means that these subproblems consider uncertainty in both the total daily RA as well as its distribution throughout the day.

The reason why we use two different RUS lies in the risk hedging requirements for two different objectives. The OF of the robust subproblem deals with financial risks associated with the total cost (soft constraint), whereas other subproblems deal with physical risks associated with the SOE equation (hard constraints). As we focus on limiting the battery operation to its feasible SOE area for all possible RA realizations, a wider RUS is assigned to the technical robust subproblems. If a different total daily RA realizes, the aggregator's profit would be somewhat lower, but the technical capability to provide the reserve would be preserved (note that this is not the case for the technical robust subproblems). The values used as parameters for soft and hard constraints are the choice of the decision maker. To illustrate this, a sensitivity analysis is provided in Subsection VI-C for the RUS input parameters of subproblems (27)–(30).

IV. MATHEMATICAL FORMULATION

First we develop the deterministic framework which is later used as a baseline for the stochastic and the robust counterparts. The nomenclature is presented in Section I above. The focus of this paper is to properly model the RA uncertainty, i.e. the uncertainty in stochastic and robust models is stemming only from RA, while prices and EV behavior are always assumed to be deterministic. The reason for such modeling is the conciseness of the paper as the RA uncertainty modeling alone is a highly complex process and any additional uncertainty modeling would make it hard to comprehend.

A. Deterministic Model – DM

The RA is usually modeled as an annual average of activations, e.g. [22], [25], [29], [30]. Similarly, our DM, which serves as the baseline, assumes average annual RA ratio of a particular reserve product. Therefore, the RA ratio is the same in all timesteps. The objective function (OF) includes five parts: cost/revenue from energy traded in the DA energy market, revenue from the power sold as FCR/aFRR capacity, V2G battery degradation cost, fast-charging cost and cost/revenue from energy withdrawn/injected as the activated FCR/aFRR (balancing energy). For brevity, the first four costs are assigned to c^{OTH} defined in eq. (3), while the costs associated to RA are assigned to c^{ACT} defined in eq. (4). Objective function is formulated as:

$$\min_{\Xi_{\mathcal{O}}} \quad (c^{\text{OTH}} + c^{\text{ACT}}); \tag{2}$$

where:

$$\begin{aligned} c^{\text{OTH}} = \sum_{t=1}^{N_t} \Big\{ \sum_{v=1}^{N_v} \big[& e_{v,t}^{\text{BUY\_DA}} \cdot C_t^{\text{DA}} - e_{v,t}^{\text{SELL\_DA}} \cdot C_t^{\text{DA}} \\ & - r_{v,t}^{\text{UP\_FCR}} \cdot CR_t^{\text{UP\_FCR}} - r_{v,t}^{\text{DN\_FCR}} \cdot CR_t^{\text{DN\_FCR}} \\ & - r_{v,t}^{\text{UP\_aFRR}} \cdot CR_t^{\text{UP\_aFRR}} - r_{v,t}^{\text{DN\_aFRR}} \cdot CR_t^{\text{DN\_aFRR}} \\ & + c_{v,t}^{\text{DEG}} + e_{v,t}^{\text{FCH}} \cdot C_{v,t}^{\text{FCH}} \big] \Big\}; \end{aligned} \tag{3}$$

$$\begin{aligned} c^{\text{ACT}} = \sum_{t=1}^{N_t} \Big\{ \sum_{v=1}^{N_v} \big[& - r_{v,t}^{\text{UP\_FCR}} \cdot A^{\text{UP\_FCR}} \cdot \Delta \cdot CA_t^{\text{UP\_FCR}} \\ & + r_{v,t}^{\text{DN\_FCR}} \cdot A^{\text{DN\_FCR}} \cdot \Delta \cdot CA_t^{\text{DN\_FCR}} \\ & - r_{v,t}^{\text{UP\_aFRR}} \cdot A^{\text{UP\_aFRR}} \cdot \Delta \cdot CA_t^{\text{UP\_aFRR}} \\ & + r_{v,t}^{\text{DN\_aFRR}} \cdot A^{\text{DN\_aFRR}} \cdot \Delta \cdot CA_t^{\text{DN\_aFRR}} \big] \Big\}; \end{aligned} \tag{4}$$

Eq. (3) sums the DA market costs consisting of energy purchase and sale as well as up and down FCR and aFRR capacity reservation, battery degradation ($c_{v,t}^{\text{DEG}}$) and EV fast charging cost (fast charged energy $e_{v,t}^{\text{FCH}}$ multiplied with price for fast charging $C_{v,t}^{\text{FCH}}$). The terms $e_{v,t}^{\text{BUY\_DA}}$ and $e_{v,t}^{\text{SELL\_DA}}$ refer to energy purchased or sold by the DA market price C_t^{DA}. The terms $r_{v,t}^{\text{UP\_FCR}}$, $r_{v,t}^{\text{DN\_FCR}}$, $r_{v,t}^{\text{UP\_aFRR}}$ and $r_{v,t}^{\text{DN\_aFRR}}$ refer to reserve capacity sold as up/down FCR/aFRR reserve at their respective prices $CR_t^{\text{UP\_FCR}}$, $CR_t^{\text{DN\_FCR}}$, $CR_t^{\text{UP\_aFRR}}$ and $CR_t^{\text{DN\_aFRR}}$. On the other hand, eq. (4) contains only the RA costs, where up RA is remunerated by the system operator (hence the minus sign), while the down RA must be payed to the system operator (hence the plus sign). The terms $A^{\text{UP\_FCR}}$, $A^{\text{DN\_FCR}}$, $A^{\text{UP\_aFRR}}$ and $A^{\text{DN\_aFRR}}$ refer to average activated reserve (balancing energy) to reserved capacity ratio which, multiplied with respective reserved capacities ($r_{v,t}^{\text{UP\_FCR}}$, $r_{v,t}^{\text{DN\_FCR}}$, $r_{v,t}^{\text{UP\_aFRR}}$ and $r_{v,t}^{\text{DN\_aFRR}}$), determine the final balancing energy volume. This energy is further multiplied with respective the RA prices ($CA_t^{\text{UP\_FCR}}$, $CA_t^{\text{DN\_FCR}}$, $CA_t^{\text{UP\_aFRR}}$ and $CA_t^{\text{DN\_aFRR}}$) to calculate the balancing energy cost or revenue.

Objective function 2 is subject to a number of constraints divided in a number of blocks for easier understanding.

$$\begin{aligned} & e_{v,t}^{\text{BUY\_DA}}, e_{v,t}^{\text{SELL\_DA}}, r_{v,t}^{\text{UP\_FCR}}, \\ & r_{v,t}^{\text{DN\_FCR}}, r_{v,t}^{\text{UP\_aFRR}}, r_{v,t}^{\text{DN\_aFRR}} \geq 0; \end{aligned} \tag{5}$$

$$\begin{aligned} & e_{v,t}^{\text{SELL\_DA}}/\Delta - e_{v,t}^{\text{BUY\_DA}}/\Delta + r_{v,t}^{\text{UP\_FCR}} + r_{v,t}^{\text{UP\_aFRR}} \\ & \leq \min(P_v^{\text{OBC\_MAX}}, P_{v,t}^{\text{CP\_MAX}}); \end{aligned} \tag{6}$$

$$\begin{aligned} & e_{v,t}^{\text{BUY\_DA}}/\Delta - e_{v,t}^{\text{SELL\_DA}}/\Delta + r_{v,t}^{\text{DN\_FCR}} + r_{v,t}^{\text{DN\_aFRR}} \\ & \leq \min(P_v^{\text{OBC\_MAX}}, P_{v,t}^{\text{CP\_MAX}}); \end{aligned} \tag{7}$$

Eq. (5) sets the six market bidding variables (purchased/sold energy and sold reserve capacity for two reserve types and

both directions) as nonnegative. Eqs. (6) and (7) limit the total charging/discharging power available for bidding to the minimum of the On-Board Charger (OBC) capacity ($P_v^{\text{OBC\_MAX}}$) and the Charging Point (CP) capacity ($P_{v,t}^{\text{CP\_MAX}}$). Δ is the timestep duration and is used to express energy as an average power during one timestep. The CP capacity ($P_{v,t}^{\text{CP\_MAX}}$) is the maximum power an EV can charge/discharge in one timestep. It originates from the input format of the EV driving/parking behaviour (explained in details in Subsection V-A). $P_{v,t}^{\text{CP\_MAX}}$ is a time-series parameter whose value depends on the EV actions in each timestep. If the EV is driving, then $P_{v,t}^{\text{CP\_MAX}}$ is zero. If the EV is parked at a CP, then $P_{v,t}^{\text{CP\_MAX}}$ is equal to the installed power capacity of that CP. In other words, (6) and (7) allocate the available power to the six market bidding variables appearing in these constraints.

$$soe_{v,t}^{\text{EV}} = SOE^{\text{T0}} \cdot B_v + e_{v,t}^{\text{OTH}} + e_{v,t}^{\text{ACT}}; \tag{8}$$

$$e_{v,t}^{\text{OTH}} = \sum\nolimits_{\tau=1}^{t} \{e_{v,\tau}^{\text{BUY\_DA}} \cdot \eta^{\text{CH}} - e_{v,\tau}^{\text{SELL\_DA}}/\eta^{\text{DCH}} - E_{v,\tau}^{\text{RUN}}/\eta^{\text{RUN}} + e_{v,\tau}^{\text{FCH}} \cdot \eta^{\text{FCH}}\}; \tag{9}$$

$$e_{v,t}^{\text{ACT}} = \sum\nolimits_{\tau=1}^{t} \Big\{\Delta \cdot \big[\eta^{\text{CH}} \cdot (r_{v,\tau}^{\text{DN\_FCR}} \cdot A^{\text{DN\_FCR}} + r_{v,\tau}^{\text{DN\_aFRR}} \cdot A^{\text{DN\_aFRR}}) - 1/\eta^{\text{DCH}} \cdot (r_{v,\tau}^{\text{UP\_FCR}} \cdot A^{\text{UP\_FCR}} + r_{v,\tau}^{\text{UP\_aFRR}} \cdot A^{\text{UP\_aFRR}})\big]\Big\}; \tag{10}$$

Eq. (8) calculates the current SOE ($soe_{v,t}^{\text{EV}}$) based on the initial SOE (B_v refers to the EV battery capacity, while SOE^{T0} is the SOE in the timestep prior to $t = 1$, expressed as a ratio toward B_v) and the energy charged/discharged to/from the EV battery until timestep t. Energy can be charged/discharged by the means of the DA market trading, driving, fast charging (taken into account with term $e_{v,t}^{\text{OTH}}$ and eq. (9)) and RA (taken into account with term $e_{v,t}^{\text{ACT}}$ and eq. (10)). Terms η^{CH}, η^{DCH}, η^{RUN} and η^{FCH} refer to efficiencies of EV slow charging, discharging, driving and fast charging, respectively. Energy consumed for driving ($E_{v,\tau}^{\text{RUN}}$) is based on the input data of the EV driving/parking behaviour and it is the second parameter defining the EV's daily behavior (the first one is $P_{v,t}^{\text{CP\_MAX}}$ explained above). In general, ($E_{v,\tau}^{\text{RUN}}$) is zero if an EV is not driving and has a positive value if an EV is on the road. $E_{v,\tau}^{\text{RUN}}$ is different for each EV type and trip as it is calculated based on the EV size (small, medium, large), trip length and vehicle the owner's average driving speed for that trip (explained in Subsection V-A). The amount of energy injected/extracted due to RA is modeled using parameters $A^{\{\text{UP/DN}\}\_\{\text{FCR/aFRR}\}} \in [0, 1]$. E.g. term $r_{v,t}^{\text{UP\_FCR}} \cdot A^{\text{UP\_FCR}} \cdot \Delta$ refers to activated up FCR reserve which can be an increase in the battery discharging or a decrease in its charging.

$$SOE^{\text{MIN}} \cdot B_v \leq soe_{v,t}^{\text{EV}} + e_{v,t+1}^{\text{BUY\_DA}} \cdot \eta^{\text{CH}} - e_{v,t+1}^{\text{SELL\_DA}}/\eta^{\text{DCH}} - \Lambda \cdot \Delta/\eta^{\text{DCH}} \cdot (r_{v,t+1}^{\text{UP\_FCR}} + r_{v,t+1}^{\text{UP\_aFRR}}) - E_{v,t+1}^{\text{RUN}}/\eta^{\text{RUN}} + e_{v,t+1}^{\text{FCH}} \cdot \eta^{\text{FCH}} \quad \forall t \in \mathcal{T}_{(t \neq N_t)}; \tag{11}$$

$$SOE^{\text{MAX}} \cdot B_v \geq soe_{v,t}^{\text{EV}} + e_{v,t+1}^{\text{BUY\_DA}} \cdot \eta^{\text{CH}} - e_{v,t+1}^{\text{SELL\_DA}}/\eta^{\text{DCH}} + \Lambda \cdot \Delta \cdot \eta^{\text{CH}} \cdot (r_{v,t+1}^{\text{DN\_FCR}} + r_{v,t+1}^{\text{DN\_aFRR}}) - E_{v,t+1}^{\text{RUN}}/\eta^{\text{RUN}} + e_{v,t+1}^{\text{FCH}} \cdot \eta^{\text{FCH}} \quad \forall t \in \mathcal{T}_{(t \neq N_t)}; \tag{12}$$

$$SOE^{\text{T0}} \cdot B_v \leq soe_{v,t}^{\text{EV}} \leq SOE^{\text{MAX}} \cdot B_v \quad \text{for } t = N_t; \tag{13}$$

$$0 \leq e_{v,t}^{\text{FCH}} \leq P^{\text{FCH\_MAX}} \cdot \Delta; \tag{14}$$

To ensure the EV batteries will be able to deliver the required reserves, their capacity is limited to SOE^{MIN} and SOE^{MAX} in eqs. (11) and (12), assuming their full activation. Eq. (11) acts as the lower bound to SOE, where only the full up RA is considered. Similarly, eq. (12) acts as the upper bound to SOE considering the full down RA. These two equations ensure that SOE remains feasible in each timestep even under full RA. Eqs. (11) and (12) are applied up to timestep $t < N_t$. Term Λ enables the decision-maker to set the desired activation duration to be considered when limiting the battery SOE. $\Lambda = 1$ indicates that the desired reserve activation duration is the same as the timestep duration. In the final timestep the conventional SOE preservation eq. (13) is applied. Fast charging is limited in (14), where $P^{\text{FCH\_MAX}}$ refers to the power capacity of a fast charger.

$$e_{v,t}^{\text{DEG}} = e_{v,t}^{\text{SELL\_DA}}/\eta^{\text{DCH}} - e_{v,t}^{\text{BUY\_DA}} \cdot \eta^{\text{CH}} + \Delta/\eta^{\text{DCH}} \cdot (r_{v,t}^{\text{UP\_FCR}} \cdot A^{\text{UP\_FCR}} + r_{v,t}^{\text{UP\_aFRR}} \cdot A^{\text{UP\_aFRR}}) - \Delta \cdot \eta^{\text{CH}} \cdot (r_{v,t}^{\text{DN\_FCR}} \cdot A^{\text{DN\_FCR}} + r_{v,t}^{\text{DN\_aFRR}} \cdot A^{\text{DN\_aFRR}}); \tag{15}$$

$$c_{v,t}^{\text{DEG}} \geq 0; \tag{16}$$

$$c_{v,t}^{\text{DEG}} \cdot B_v \geq C_v^{\text{B}} \cdot \big[-D_1^{\text{B}} \cdot B_v + D_2^{\text{B}} \cdot e_{v,t}^{\text{DEG}} + D_3^{\text{B}} \cdot (B_v - soe_{v,t}^{\text{EV}})\big]; \tag{17}$$

$$c_{v,t}^{\text{DEG}} \cdot B_v \geq C_v^{\text{B}} \cdot D_4^{\text{B}} \cdot e_{v,t}^{\text{DEG}}. \tag{18}$$

Li-ion batteries are prone to degradation, especially when cycled often. Incorporating degradation cost in the OF may reduce the battery charging/discharging actions not related to driving. The degradation is taken into account when discharging in the DA market or through RA in eq. (15). Term $e_{v,t}^{\text{DEG}}$ calculates the net energy discharged from each EV in each timestep. Eq. (16) defines $c_{v,t}^{\text{DEG}}$ as a positive variable. Eqs. (17) and (18) bound and calculate the V2G discharging degradation cost. These constraints are a linearized form of the degradation model from [33]. Term C_v^{B} is investment cost of the EV battery, while terms D_1^{B}, D_2^{B}, D_3^{B} and D_4^{B} are strictly numerical parameters derived by linearizing the battery degradation curve [34].

The above constraints (5)–(18) apply for $\forall v \in \mathcal{V}$ and $\forall t \in \mathcal{T}$, except for eqs. (11)–(12), which are not valid for the last period, and for (13), which is valid for the last period only.

B. Stochastic Model – SM

The SM differs from the DM in the definition of the RA ratio. While the DM uses a single value for all timesteps, the SM uses the RA ratio as a time-dependable parameter obtained from historic data (details on how these data are used is explained in Section III). The RA parameters $A_{s,t}^{\{\text{UP/DN}\}\_\{\text{FCR/aFRR}\}}$ and the associated variables c_s^{ACT}, $e_{s,v,t}^{\text{ACT}}$, $soe_{s,v,t}^{\text{EV}}$, $e_{s,v,t}^{\text{DEG}}$, $c_{s,v,t}^{\text{DEG}}$ gain an additional index s in the SM as compared to the DM. The DM is thus reformulated using eqs. (19)–(22). Eqs. in (20) are identical as in the DM, while the SM instances of eqs. (21) and (22) are additionally valid $\forall s \in \mathcal{S}$. Term P_s stands for scenario probability.

Objective function:

$$\min_{\Xi_{\mathcal{O}}} [P_s \cdot \sum\nolimits_{s=1}^{N_s} (c_s^{\text{OTH}} + c_s^{\text{ACT}})]; \tag{19}$$

subject to:

$$(5) - (7); \tag{20}$$

$$(4), (10), (15), \quad \forall s \in \mathcal{S}; \tag{21}$$

$$(3), (8) - (9), (11) - (14), \\ (16) - (18), \quad \forall s \in \mathcal{S}. \tag{22}$$

C. Robust Model – RM

In the RM, the RA quantities are uncertain parameters ($a_{v,\tau,t}^{\text{UP\_FCR}}$, $a_{v,\tau,t}^{\text{DN\_FCR}}$, $a_{v,\tau,t}^{\text{UP\_aFRR}}$, $a_{v,\tau,t}^{\text{DN\_aFRR}}$) whose boundaries are defined by the US defined in eqs. (31)–(38) with parameters resulting from the probabilistic analysis in Section III. OF of the RM, stated in eq. (23), minimizes the total operating costs for the worst-case RA, i.e. maximizing the RA throughout the day, which is stated in subproblems eqs. (26)–(30). The subproblem stated in eq. (26) is the OF of the robust subproblem, while the subproblems stated in eqs. (27)–(30) are the robust subproblems related to the technical constraints containing uncertain parameters. Such min-max structure cannot be solved directly and an appropriate RM reformulation described in [38] is used.

The initial formulation of the RM is presented in Section IV-C1, while the US is presented in Section IV-C2. Using the duality theory, all the subproblems are recast as duals and merged with the rest of the constraints creating the final problem presented in Section IV-C3.

1) Initial Formulation:

Objective function:

$$\min_{\Xi_{\mathcal{O}}} \quad (z) \tag{23}$$

is subject to:

$$(3), (5) - (7), (9), (14) - (18); \tag{24}$$

$$(4), (10); \tag{25}$$

$$\max_{\Xi_{\mathcal{A}}} (c^{\text{ACT}}) \leq z - c^{\text{OTH}}; \tag{26}$$

$$\max_{\Xi_{\mathcal{A}}} (-e_{v,t}^{\text{ACT}}) \leq B_v \cdot (SOE^{\text{T0}} - SOE^{\text{MIN}}) \\ -\Lambda \cdot \Delta / \eta^{\text{DCH}} \cdot (r_{v,t+1}^{\text{UP\_FCR}} + r_{v,t+1}^{\text{UP\_aFRR}}) + e_{v,t+1}^{\text{OTH}}; \tag{27}$$

$$\max_{\Xi_{\mathcal{A}}} (e_{v,t}^{\text{ACT}}) \leq B_v \cdot (SOE^{\text{MAX}} - SOE^{\text{T0}}) \\ -\Lambda \cdot \Delta \cdot \eta^{\text{CH}} \cdot (r_{v,t+1}^{\text{DN\_FCR}} + r_{v,t+1}^{\text{DN\_aFRR}}) - e_{v,t+1}^{\text{OTH}}; \tag{28}$$

$$\max_{\Xi_{\mathcal{A}}} (e_{v,t}^{\text{ACT}}) \leq B_v \cdot (SOE^{\text{MAX}} - SOE^{\text{T0}}) - e_{v,t}^{\text{OTH}}; \tag{29}$$

$$\max_{\Xi_{\mathcal{A}}} (-e_{v,t}^{\text{ACT}}) \leq e_{v,t}^{\text{OTH}}. \tag{30}$$

The OF of the RM stated in eq. (23) minimizes the total cost (z) of an EV fleet. Eqs. (24) are the same as in the DM, while the uncertain parameters appear in constraints containing RA variables, grouped under eq. (25). Eqs. (25) are similar as in the DM, but the fixed RA parameter is replaced with the uncertain one. The OF and each constraint containing terms with uncertain parameters from eq. (25) are observed as independent maximization subproblems stated in eqs. (26)–(30). OF of the DM stated in eq. (2) is reformulated to its robust counterpart presented in eqs. (23) and (26). Eqs. (11)–(13) are adequately reformulated into eqs. (27)–(30). Note that the SOE balance eq. (8) is already incorporated into the aforementioned eqs. and that SOE as a variable does not exist in the robust counterpart. Eqs. (27) and (28) are valid for $\forall v \in \mathcal{V}$ and $\forall t \in \mathcal{T}_{t \neq N_t}$, while the eqs. (29) and (30) are valid for $\forall v \in \mathcal{V}$ and for $t = N_t$.

2) Uncertainty Set:

Subproblems defined by eqs. (26)–(30) are valid $\forall \ (a_{v,\tau,t}^{\text{UP\_FCR}}, a_{v,\tau,t}^{\text{DN\_FCR}}, a_{v,\tau,t}^{\text{UP\_aFRR}}, a_{v,\tau,t}^{\text{DN\_aFRR}}) \in \mathcal{A}$, where $\mathcal{A}$ is the following RUS:

$$\mathcal{A} = \big\{ a_{v,\tau,t}^{\text{UP\_FCR}}, a_{v,\tau,t}^{\text{DN\_FCR}}, a_{v,\tau,t}^{\text{UP\_aFRR}}, a_{v,\tau,t}^{\text{DN\_aFRR}} \quad | \\ a_{v,\tau,t}^{\text{UP\_FCR}}, a_{v,\tau,t}^{\text{DN\_FCR}} \geq 0; \tag{31}$$

$$a_{v,\tau,t}^{\text{UP\_FCR}} + a_{v,\tau,t}^{\text{DN\_FCR}} \leq A^{\text{MAX\_FCR}} : \omega_{v,\tau,t}^{\text{FCR}}; \tag{32}$$

$$\sum\nolimits_{\tau=1}^{t} a_{v,\tau,t}^{\text{UP\_FCR}} \leq (\Gamma^{\text{UP\_FCR}} - 1) \cdot I_t + 1 : \mu_{v,t}^{\text{FCR}}; \tag{33}$$

$$\sum\nolimits_{\tau=1}^{t} a_{v,\tau,t}^{\text{UP\_FCR}} \geq \Upsilon^{\text{UP\_FCR}} \cdot I_t : \nu_{v,t}^{\text{FCR}}; \tag{34}$$

$$\sum\nolimits_{\tau=1}^{t} a_{v,\tau,t}^{\text{DN\_FCR}} \leq (\Gamma^{\text{DN\_FCR}} - 1) \cdot I_t + 1 : \psi_{v,t}^{\text{FCR}}; \tag{35}$$

$$\sum\nolimits_{\tau=1}^{t} a_{v,\tau,t}^{\text{DN\_FCR}} \geq \Upsilon^{\text{DN\_FCR}} \cdot I_t : \chi_{v,t}^{\text{FCR}}; \tag{36}$$

$$(31)\text{–}(36) \text{ are analogous for aFRR.} \big\}; \tag{37}$$

$$(31)\text{–}(37) \text{ are similar for } (26)\text{–}(30). \tag{38}$$

General explanation. The RUS presented in eqs. (31)–(36) applies to the *FCR* service and the subproblem stated in eq. (27) as an exemplary formulation. The eqs. for aFRR are analogous to eqs. (31)–(36), as indicated in eq. (37). For other subproblems the formulations are similar to eqs. (31)–(37), as indicated in eq. (38). The form is the same and the differences are in the indexations of summations and dual variables. Those formulations are omitted due to succinctness of the paper. Please note that each of the five subproblems in eqs. (26)–(30) contains one US $\mathcal{A}$ with its own four uncertain parameters ($a_{v,\tau,t}^{\text{UP\_FCR}}, a_{v,\tau,t}^{\text{DN\_FCR}}, a_{v,\tau,t}^{\text{UP\_aFRR}}, a_{v,\tau,t}^{\text{DN\_aFRR}}$). In total, our master problem has $5 \cdot 4 = 20$ uncertain parameters. Following this reasoning, each of the eqs. (31)–(36) can have different US parameters on the right-hand-side (the ones used in this paper are presented in Table I) and have different dual variables. The dual variables of the US equations are provided after a colon on the right side of equations ($\omega_{v,\tau,t}^{\text{FCR}}$, $\mu_{v,t}^{\text{FCR}}$, $\nu_{v,t}^{\text{FCR}}$, $\psi_{v,t}^{\text{FCR}}$, $\chi_{v,t}^{\text{FCR}}$).

Explanation of the RUS formulation for *FCR* service and subproblem stated in eq. (27). Eq. (31) sets all uncertain parameters ($a_{v,\tau,t}^{\text{UP\_FCR}}, a_{v,\tau,t}^{\text{DN\_FCR}}$) as non-negative. Eq. (32) limits the sum of UP and DN FCR activation variables in each timestep using parameter $A^{\text{MAX\_FCR}}$. This equation is visualised as green or cyan line in Figures 1a and 1b. Values of A^{MAX} used in this paper are shown in Section III, Table I. This constraint limits both the individual UP and DN activations, as well as their summation. This stems from the historic data analysis that indicates if the activation in one direction is high, the activation in the other direction will be low and vice versa. Eqs. (33)–(36) consider the daily sums of the RA ratios (daily specific balancing energy). Eqs. (33) and (35) (eqs. (34) and (36)) state that total RA ratio up to a certain timestep must be lower (higher) than its limiting value on the right-hand-side.

Parameters Γ and Υ stand for the upper and lower limits of the daily sums of RA ratios and they are defined in Section III, Table I. Index t stands for the observed timestep, while the auxiliary index τ iterates through all the previous timesteps to sum the RA variables. Parameter I_t on the right-hand-side represents a uniformly distributed range $\in [0,1]$ through time. At timestep $t=1$ it equals 0, in $t=N_t/2$ it equals 0.5, while in $t=N_t$ it equals 1, as shown in Figure 3. The right-hand-side in $t=N_t$ equals to Γ or Υ, while they are linearly scaled with I_t in the previous timesteps. In $t=1$ those constraints are not binding as I_t is 0. The right-hand-side of eqs. (33)–(36) are shown in Figure 3, where the blue and red (yellow and green) lines represent limits in each step t for $\sum_{\tau=1}^{t} a_{v,\tau,t}^{\text{UP\_FCR}}$ ($\sum_{\tau=1}^{t} a_{v,\tau,t}^{\text{DN\_FCR}}$).

3) Final Formulation:

Objective function:

$$\min_{\Xi_{\mathcal{O}}} \quad (z) \tag{39}$$

subject to:

$$(3),(5)-(7),(9),(14)-(18); \tag{40}$$

$$(4),(10); \tag{41}$$

$$\begin{aligned} &A^{\text{MAX\_FCR}} \cdot \sum_{\tau=1}^{t} \omega_{v,\tau,t}^{\text{FCR}} \\ &+\left[(\Gamma^{\text{UP\_FCR}}\text{-}1)\cdot I_t{+}1\right]\cdot\mu_{v,t}^{\text{FCR}}+\Upsilon^{\text{UP\_FCR}}\cdot I_t\cdot\nu_{v,t}^{\text{FCR}} \\ &+\left[(\Gamma^{\text{DN\_FCR}}\text{-}1)\cdot I_t{+}1\right]\cdot\psi_{v,t}^{\text{FCR}}+\Upsilon^{\text{DN\_FCR}}\cdot I_t\cdot\chi_{v,t}^{\text{FCR}} \\ &A^{\text{MAX\_aFRR}} \cdot \sum_{\tau=1}^{t} \omega_{v,\tau,t}^{\text{aFRR}} \\ &+\left[(\Gamma^{\text{UP\_aFRR}}\text{-}1)\cdot I_t{+}1\right]\cdot\mu_{v,t}^{\text{aFRR}}+\Upsilon^{\text{UP\_aFRR}}\cdot I_t\cdot\nu_{v,t}^{\text{aFRR}} \\ &+\left[(\Gamma^{\text{DN\_aFRR}}\text{-}1)\cdot I_t{+}1\right]\cdot\psi_{v,t}^{\text{aFRR}}+\Upsilon^{\text{DN\_aFRR}}\cdot I_t\cdot\chi_{v,t}^{\text{aFRR}} \\ &\leq B_v\cdot(SOE^{\text{T0}}-SOE^{\text{MIN}}) \\ &-\Lambda\cdot\Delta/\eta^{\text{DCH}}\cdot(r_{v,t+1}^{\text{UP\_FCR}}+r_{v,t+1}^{\text{UP\_aFRR}})+h_{v,t+1}^{\text{NRA}}; \end{aligned} \tag{42}$$

$$\begin{aligned} &\omega_{v,\tau,t}^{\text{FCR}}+\mu_{v,t}^{\text{FCR}}+\nu_{v,t}^{\text{FCR}} \geq \\ &\Delta/\eta^{\text{DCH}}\cdot r_{v,\tau}^{\text{UP\_FCR}} \quad : a_{v,\tau,t}^{\text{UP\_FCR}}; \end{aligned} \tag{43}$$

$$\begin{aligned} &\omega_{v,\tau,t}^{\text{FCR}}+\psi_{v,t}^{\text{FCR}}+\chi_{v,t}^{\text{FCR}} \geq \\ &-\Delta\cdot\eta^{\text{CH}}\cdot r_{v,\tau}^{\text{DN\_FCR}} \quad : a_{v,\tau,t}^{\text{DN\_FCR}}; \end{aligned} \tag{44}$$

$$\omega_{v,\tau,t}^{\text{FCR}},\mu_{v,t}^{\text{FCR}},\psi_{v,t}^{\text{FCR}}\geq 0; \tag{45}$$

$$\nu_{v,t}^{\text{FCR}},\chi_{v,t}^{\text{FCR}}\leq 0; \tag{46}$$

$$(43)\text{–}(46) \text{ are analogous for aFRR}; \tag{47}$$

$$(42)\text{–}(47) \text{ are similar for } (26)\text{–}(30). \tag{48}$$

General explanation. The final robust formulation (eqs. (39)–(48)) contains an exemplary subproblem of eq. (27) and FCR service. Eqs. (39)–(41) are the same as in the RI formulation. Eqs. (42)–(46) are related to the exemplary subproblem and service. Eq. (47) spreads the model over the aFRR dual constraints and they are the same as for the FCR reserve (only with the aFRR variables and parameters). Eq. (48) spreads the model on subproblems defined with eqs. (26), (28)–(30). Equations for those subproblems are of the same form but with the differences in the indexations of summations and dual variables. Those formulations are omitted due to succinctness of the paper.

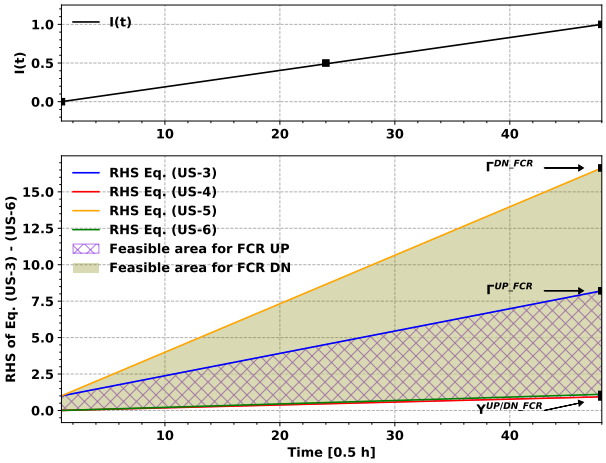

Fig. 3. Right-hand-side visualization for uncertainty set parameter evolution through time

Explanation of the final robust formulation for *FCR* service and subproblem stated in eq. (27). Eqs. (42) represents a strong duality equation including both the FCR and aFRR services in both directions. At the left-hand-side the dual variables ($\omega_{v,\tau,t}^{\text{FCR}}$, $\mu_{v,t}^{\text{FCR}}$, $\nu_{v,t}^{\text{FCR}}$, $\psi_{v,t}^{\text{FCR}}$, $\chi_{v,t}^{\text{FCR}}$) are multiplied with their related US parameters ($A^{\text{MAX\_FCR}}$, $\Gamma^{\text{UP\_FCR}}$, $\Upsilon^{\text{UP\_FCR}}$, $\Gamma^{\text{DN\_FCR}}$, $\Upsilon^{\text{DN\_FCR}}$), while the right-hand-side is forwarded from eq. (27). Dual constraints for uncertain parameters $a_{v,\tau,t}^{\text{UP\_FCR}}$ and $a_{v,\tau,t}^{\text{DN\_FCR}}$ are presented in eqs. (43) and (44), respectively. The left-hand-side contains all the related dual variables and their linear combination, while the right-hand-side stems from the objective function of subproblem stated in eq. (27). Eqs. (45) and (46) set the dual variables as non-negative and non-positive, respectively. Those constrains arise from the inequality directions from the eqs. (32)–(36).

Eq. (42) applies $\forall t\in\mathcal{T}$ and $\forall v\in\mathcal{V}$, while eqs. (43)–(46) additionally apply $\forall\tau\in\mathcal{T},\tau<t$.

V. Case Studies

The case study employs three models: the DM with average annual RA, the SM with 10 ex-ante RA scenarios (scenario examples are given Figure 2) and the RM with the RUS based on the real balancing data. The outcome of the models are DA schedules, whose quality is assessed using one hundred historical RA scenarios in ex-post analysis.

The optimization model was run in Fico Xpress environment (Xpress IVE version 1.24.26 64 bit) on Intel Core i7-6700 CPU at 3.4 GHz with 32 GB RAM. All the simulations were solved using the Newton barrier method which demonstrated faster execution as compared to the simplex method, both for the stochastic and the robust model.

A. Input Parameters

The EV driving/parking behaviour was consolidated from the European driving study [4], [36], and [37] where six EU countries have been observed. The data was first restructured to represent 5-min EV driving/parking behaviour.

For each EV and each half-hourly period, two input parameters are required: the EV driving consumption, $E_{v,t}^{\text{RUN}}$ in eq. (8), and maximum CP power, $P_{v,t}^{\text{CP\_MAX}}$ in eqs. (6) and

(7). Driving/parking timelines from the JRC study [4], [36], [37] are used for each half-hour for each EV both for the energy that the EVs discharge for motion while driving ($E_{v,\tau}^{\text{RUN}}$) and for the boundaries for the EVs' slow charging/discharging ($P_v^{\text{OBC\_MAX}}$) while parked. An example of a final half-hourly timetable for one EV is provided in Table II. Column *Status* is zero when parked and one when driving, $E_{v,\tau}^{\text{RUN}}$ is the consumed energy during the trip, $P_v^{\text{OBC\_MAX}}$ is power limit for slow charging and *Parking* is the parking type from the JRC study. The observed vehicle is parked at home until half-hour 8, then it travels in half-hours 10-13 and is parked at a private parking at half-hour 14. Parking types were used to assign instantaneous CP capacity, i.e. to choose the CP type. In total there are 11 parking types in the JRC study but we derived three CP types from them for brevity: low (3.7 kW), medium (7.4 kW) and high (11 kW). This is presented in Table III. Vehicle type, trip length and average trip speed were used as inputs to calculate the EV consumption while driving, consolidated in parameter ($E_{v,\tau}^{\text{RUN}}$).

TABLE II
DRIVING/PARKING FORECAST EXAMPLE

Half-hour	Status	$E_{v,\tau}^{\text{RUN}}$ [kWh]	$P_v^{\text{OBC\_MAX}}$ [kW]	Parking
8	0	0	3.7	2
9	0	0	3.7	2
10	1	1.62	2.78	2
11	1	6.48	0	0
12	1	6.48	0	0
13	1	4.32	2.47	6
14	0	0	7.4	6
15	0	0	7.4	6

The data-set for France was used with the total of 581 EVs divided into three types based on vehicle type (battery capacity, OBC size, fleet share): small (20 kWh, 3.7 kW, 30%), medium (40 kWh, 7.4 kW, 40%) and large (60 kWh, 11 kW, 30%). The total fleet capacity is 23.08 MWh, and the total OBC power is 4.26 MW. The EV battery capacity limits are $SOE^{\text{T0}} = 0.6$, $SOE^{\text{MAX}} = 1$, $SOE^{\text{MIN}} = 0.2$.

B. Characteristic Days

The models are tested on four characteristic days:

- *Day 1* – energy price curve with low daily volatility and low FCR capacity price,
- *Day 2* – energy price curve with low daily volatility and high FCR capacity price,
- *Day 3* – energy price curve with high daily volatility and low FCR capacity price,
- *Day 4* – energy price curve with high daily volatility and high FCR capacity price.

The prices are taken from the French electricity exchange and transmission system operator websites for 2018-2019 [35]. The aFRR price is the same in all four days as its price in France is regulated.

C. Case Studies Introduction

When the reserve is scheduled in the DA, its activation in real-time affects the SOE of a particular EV. If the RA at a certain timestep is such that it steers the SOE to its limits and disables the adherence of the planned DA schedule, the aggregator must redispatch this EV by trading in subsequent intraday/balancing markets to backtrack the SOE to its DA-planned value. In reality, the SOE limits cannot be violated as any kind of charging or discharging would stop if the EV reaches its battery limits. However, in the ex-post analysis carried out in Section VI the violation of the SOE limits is used as an indicator when the EV DA scheduling algorithm incorrectly models the RA uncertainty. The goal of the proposed algorithms is to ensure that even without trading in subsequent markets, or any other kind of redispatching, the RA does not cause infeasible SOE levels and inability to provide the promised services. Please note that converting the mentioned indicators to financial values or penalization would require detail modeling of the intraday and balancing markets, imbalance settlement and unsupplied reserve penalization fee, which would broaden the scope of the paper without the effect on the objective of this research, which is the exact modeling of reserve activation uncertainty. Therefore, we use the following terms as validation indicators of inadequate uncertainty modeling: minimum or maximum SOE of individual EV, number of EVs within the fleet with SOE outside its bounds, total energy outside the SOE bounds for the whole EV fleet.

TABLE III
PARKING PLACE (PP) DATA

PP Type	PP Name	CP Type
1	Own private space at home	1
2	Own private garage at home	1
3	On a drive way	1
4	Park-and-ride car park	2
5	Reserved firm/work parking area	2
6	Open air private parking area	2
7	Public garage	2
8	Open air private parking area	3
9	Private garage	3
10	Kerbside, regulated parking	3
11	Kerbside, regulated parking	3

VI. RESULTS AND DISCUSSION

Using the RUS parameters from Table I the main analysis is performed to compare the three observed models. A detailed analysis of the daily schedules/profiles and EVs violating the constraints is shown in Section VI-A. The relevant results are given as timeseries in Figures 4–6 for Day 1. The Section VI-B expands the analysis on four characteristic days using the aggregated results presented in Table IV.

Section VI-C focuses only on RM and Day 1 to provide a sensitivity analysis on the input parameters for the RUS. The sensitivity analysis is done only for the RUS inputs of subproblems (43)–(46), while the inputs for (42) are held fixed (the values from the Table I). The results are presented as bar graphs for different RUS parameters and shown in Figure 7.

A. Day-ahead Plans – Day 1

Figures 4–6 show the results of the three models. Subfigures to the left show the DA schedules and subfigures to the right show how those plans affect the SOE constraints of the EV fleet. The DM schedules maximum aFRR (at higher price as compared to the FCR) in both directions plus it schedules a large amount of DA charging energy to compensate for

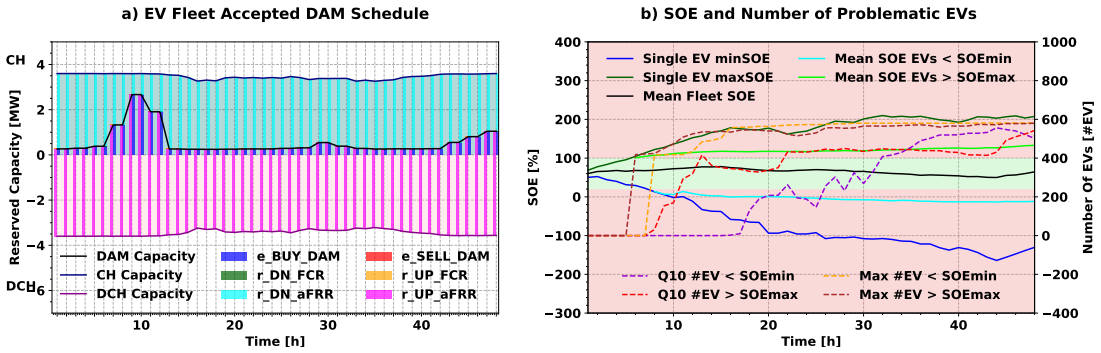

Fig. 4. Results of the deterministic model – day 1

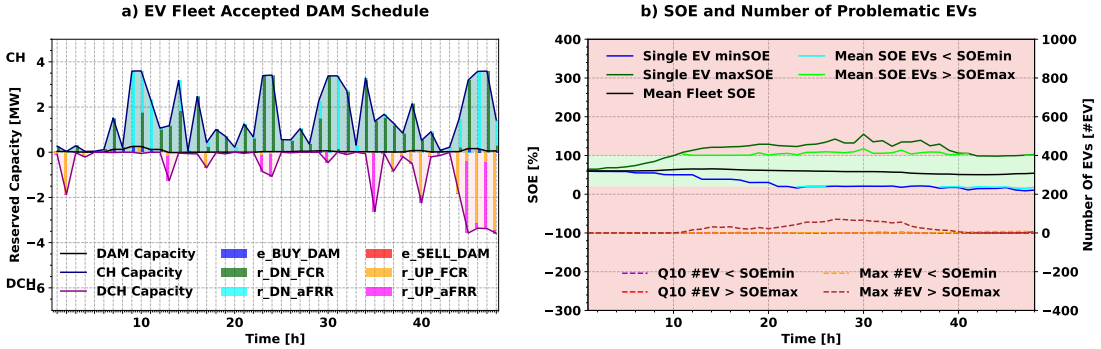

Fig. 5. Results of the stochastic model – day 1

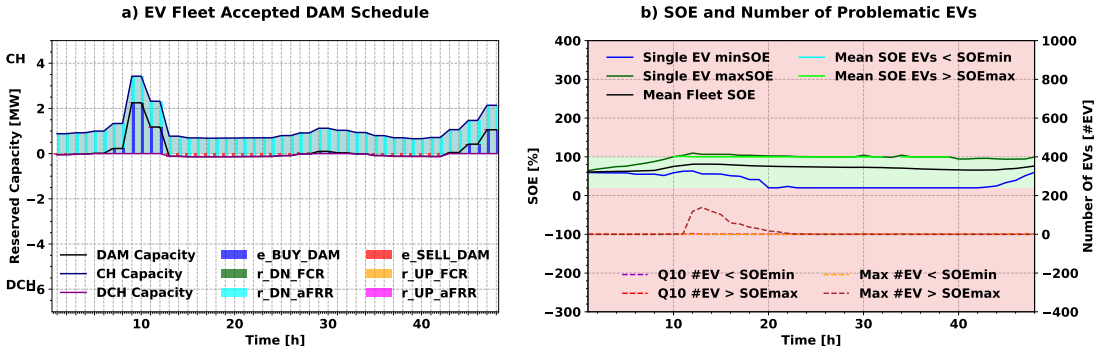

Fig. 6. Results of the robust model – day 1

the missing energy. Due to a high amount of the scheduled reserves, a high number of EVs end up with their SOE limits violated in both directions (up to 581) and by a significant margin (up to -164% and 210%). In Figure 4b) the solid lines denote SOE in % and the dashed lines represent the number of EVs outside the limits in the worst-case scenario *Max* and excluding the 10% of the worst scenarios *Q10*.

The SM adjusts the reserve schedule to its ex-ante scenarios and results in variable reserve schedules where both the FCR and the aFRR are utilized in both directions, as shown in Figure 5. The down reserve is scheduled more frequently to avoid charging in the DA energy market. Even though the aFRR reserve is better priced, the FCR is scheduled more frequently since it is less stochastic. The number of EVs beneath the SOE^{MIN} level is negligible during the entire day, whereas during the daytime a certain amount of EVs can surpass SOE^{MAX} (up to 71 EVs and up to 155% of SOE).

The RM adjusts the reserve schedule to find a trade-off between the OF value and the worst-case RA. It schedules the reserve rather uniformly through the day and selects only aFRR in down direction (higher price than FCR), as presented in Figure 6. DA energy charging and discharging is utilized to create the optimal working point for each EV, i.e. to maximize reserve provision for the worst-case realization of uncertainty. There are almost no EVs surpassing SOE^{MAX}. The morning peak of such EVs is visible in Figure 6b), but their SOE is only slightly above SOE^{MAX} (110% as compared to 155% for the SM and 210% for the DM). The reason for this lies in the linear representation of $I(t)$ to model the activated energy. None of the EVs have an SOE beneath SOE^{MIN} for the RM versus a negligible number for the SM (8 EVs down to -8.83%) and a significant number for the DM (556 EVs down to -164%). It can be concluded that both the SM and the RM compromise between the revenue and the uncertainty but in their unique way and that the EVs rarely surpass their SOE limits.

TABLE IV
AGGREGATE RESULTS FOR TWO REFERENCE DAYS BASED ON 100 EX-POST SCENARIOS SIMULATION

Observed Results			*Day 1*			*Day 2*			*Day 3*			*Day 4*		
			DM	SM	RM	DM	SM	RM	DM	SM	RM	DM	SM	RM
I)	Min Cost	[10^3 €]	**-2.51**	-0.20	0.01	**-1.86**	-0.59	-0.05	**-2.57**	-0.21	0.04	**-1.87**	-0.60	-0.03
	Max Cost	[10^3 €]	**-0.07**	0.28	0.34	**-0.29**	0.09	0.38	**-0.03**	0.31	0.34	**-0.29**	0.12	0.37
II)	Min SOE	[%]	-164.11	8.83	**20.00**	-37.78	4.99	**20.00**	-141.48	6.70	**20.00**	-36.81	4.76	**20.00**
	Max ΣSOE $<$	[MWh]	25.12	0.01	**0.00**	4.34	0.02	**0.00**	23.97	0.01	**0.00**	3.98	0.03	**0.00**
	Max #EV $<$	[#]	581	8	**0**	523	21	**0**	581	7	**0**	520	26	**0**
III)	Max SOE	[%]	209.89	154.97	**109.60**	190.26	176.93	**106.84**	213.27	149.01	**111.78**	188.53	181.31	**109.37**
	Max ΣSOE $>$	[MWh]	16.15	0.27	**0.15**	12.95	0.50	**0.31**	16.15	0.36	**0.22**	12.41	0.60	**0.10**
	Max #EV $>$	[#]	580	**71**	139	572	**307**	420	580	**89**	170	570	457	**105**

B. Summarized Results – All Days

The results shown in Table IV are separated into three major segments, providing the statistics on: I) the realized costs, II) the EVs whose SOE is theoretically lower than SOE^{MIN}, III) the EVs whose SOE is theoretically higher than SOE^{MAX}. Shaded cells highlight the worst results for a specific reference day, while the best results are in bold text.

As seen in Figures 4–6, the DM provides maximum possible reserve at the expense of the provision infeasibility. Thus, it displays the lowest costs in segment I of Table IV. *Min Cost* for the DM ranges from -2570 to -1860 €, while *Max Cost* is in between -290 and -30 €. The RM, due to its strict RUS on the SOE limits but loose RUS on the OF, provides the highest cost solution. *Min Cost* for the RM is always higher than -50 € and *Max Cost* is always higher than 340. However, the DM would suffer greatly from the penalties related to the energy and reserve redispatching in the real time, whereas the RM would be mostly intact by them, i.e. it would be robust to the risks of not being able to provide the scheduled services. The SM is in between these two models, with *Min Cost* ranging from -200 to -600 € and *Max Cost* in between 90 and 310 €.

In segments II) and III) of Table IV, *Min/Max* parameters refer to the worst realization of the observed parameter. In segment II), *Min SOE* corresponds to the lowest EV SOE realized in the ex-post analysis. The lowest *Min SOE* is always achieved for the DM with -164.11% in the worst characteristic day (Day 1). The SM yields better results as compared to the DM, but *Min SOE* is still underneath the allowable limits of 20% (for the worst reference day – Day 4 it is 4.76%). The lowest SOE in the RM is just at the lower SOE limit, i.e. 20%, meaning it does not violate the SOE^{MIN} limit in any of the observed reference days. *Max* Σ*SOE*$<$ indicates the overall energy below SOE^{MIN} for the entire fleet in one timestep. The DM results in highest energy mismatch, going as high as 25 MWh of unsupplied energy, the SM is in range of several dozens kWh, and the RM is without such energy mismatch. *Max #EV*$<$ indicates the number of EVs with SOE falls below SOE^{MIN} in the worst case. In the DM, all or almost all EVs (520-581) suffer from the SOE lower than SOE^{MIN} . The SM schedule results in up to 26 EVs below SOE^{MIN}, whereas the RM model does not suffer from this issue.

The parameters from segment III) in Table IV are analogous to those from segment II), they just refer to the EVs' upper SOE limits. *Max SOE* is the highest for the DM (up to 213.27%), closely followed by the SM (up to 181.31%), and by far the lowest for the RM (up to 111.78%). High *Max* $\Sigma>$*SOE* values are achieved for the DM (up to 16.15 MWh), whereas the SM and RM are in the range of several hundreds kWh (RM lower for all characteristic days). Maximum number of EVs above SOE^{MAX} (*Max #EV*$>$) is extremely high for the DM (almost all EVs, 570-580), but also relatively high for the SM and RM as well (up to 457 and 420, respectively). For the first three characteristic days the SM even achieves better results than the RM. However, these numbers should be observed in relation to the maximum value of SOE. The high number of EVs above SOE^{MAX} for the RM means high number of EVs whose SOE is just slightly above SOE^{MAX}.

Regarding the computational efficiency, the DM is solved in around 30 seconds (day 1: 27.67 s, day 2: 29.03 s, day 3: 27.59 s, and day 4: 30.58 s). The SM is solved in 10-20 minutes (day 1: 867.99 s, day 2: 541.75 s, day 3: 1288.41 s, and day 4: 573.48 s), while the RM is solved in around 10 minutes (day 1: 555.54 s, day 2: 545.52 s, day 3: 6387.20 s, and day 4: 650.50 s). The SM and RM are much slower than the DM, but for the DA requirements the computational time is satisfactory. The RM is more constant, with solving time around 10 minutes, while the solving time for SM depends on input parameters.

To conclude this results analysis, from the perspective of the SOE limits violation the RM provides the best solution closely followed by the SM. The DM is prone to high deviations in the actual realization of RA.

C. Sensitivity Analysis - Day 1

Sensitivity analysis for the robust model RUS input parameters was preformed for Day 1. Five test RUS are defined for subproblems (43)–(46) for the daily sums of the RUS parameters (Υ and Γ):

- Q0 - max/min data, the same as in Table I,
- Q1 - neglecting 1% of the worst activations,
- Q5 - neglecting 5% of the worst activations,
- Q10 - neglecting 10% of the worst activations,
- Q25 - neglecting 25% of the worst activations.

The maximum achieved RA ratio (A^{MAX}) for each test RUS was held fixed as in Table I. All RUS inputs for subproblem (42) are also held fixed for each test RUS as in Table I.

The goal of this analysis is to check whether the RUS constraints can be loosened to increase profit by providing more reserve but without sacrificing the feasibility of the EV conditions in the real-time. Figure 7 shows four types of indicators: min/max individual SOE (right axis in %) and min/max fleet-wise energy exceeding the SOE limits (left axis in MWh).

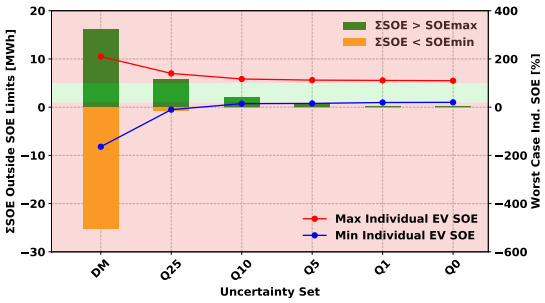

Fig. 7. Comparison of validation indicators for tested cases

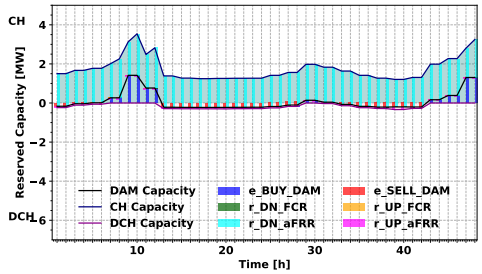

Fig. 8. Electric vehicle accepted day-ahead schedule for the test case neglecting 10% of uncertainty

The QO UC shows a conservative solution where the entire range of uncertainty is considered and no infeasible SOE can appear in real-time (the daily profile is visible on Figure 6). If a portion of uncertainty is neglected, more issues appear in the real-time. By neglecting more uncertainty, more potential issues arise, as seen for cases Q1–Q25 in Figure 7. For this characteristic day even the results for Q10 seem sufficiently risk-free. Even if we neglect 25% of uncertainty, as in Q25, the results are still more resistant to uncertainty than in the DM. On the other side, neglecting uncertainty leads to more allocated reserves, meaning that profits can be poured into the aggregators pockets. The scheduling result for the Q10 test RUS is shown in Figure 8. Compared to Q0 (Figure 6), Q10 allocates more reserve. In average, the Q0 RUS schedules 2.96 x 10^{-4} MW aFRR UP and 1.62 MW aFRR DN, while the Q10 RUS schedules 0.13 MW aFRR UP and 2.86 MW aFRR DN reserve.

The value of the robust model is that the decision maker can choose its preferred level of conservativness. A risk-prone aggregator can take liberal decisions gambling with the real-world conditions such as Q25, while the risk-averse will be satisfied with Q0 or Q1 input setup.

VII. Conclusion

The paper brings a novel approach to modelling uncertainty of scheduling the automatic reserves activation (both aFRR and FCR) in European markets. It proposes stochastic- and robust-based optimization models, where scenarios and uncertainty sets are based on an analysis of the real-world historical data. The existing deterministic model fails to properly accommodate the uncertain aspects of the reserve activation. The presented case study clearly demonstrates the advantages of the proposed approaches.

Although claiming high DA benefits, the deterministic model results in extreme individual violations of the EVs' battery SOE limits, ranging from -160% to above 200% SOE. Additionally, it results in high fleet-level deviations, from 25 MWh above SOE^{MAX} to 15 MWh below SOE^{MIN}. These deviations would, in reality, manifest as an inability to provide the scheduled DA energy, activated reserve energy or driving energy. The stochastic and robust formulations decrease the risks related to infeasible reserve activations. Minimum and maximum individual SOE levels achieved in the stochastic model are 4.76% and 181.31% of SOE and in the robust model 20% and 111.78% SOE. At the fleet level, energy levels below SOE^{MIN} are negligible, while levels above SOE^{Max} are in the range of dozens of kWh. Both formulations are technology-agnostic and can be implemented in other algorithms (redispatch measures, other markets, adaptive robust algorithms, etc.) and paired with price, behavior or bid acceptance uncertainties. However, the robust model is more flexible and there are many improvements to be made on top of the the features presented in this paper, e.g. it can be further tailored for specific needs tightening or relaxing specific RUS parameters.

The proposed paper observed only the reserve activation uncertainty. Including the uncertainty on prices and EV behaviour could further improve the bidding outcomes. The risk associated with overforcasting or underforecasting the price, and therefore the risks in terms of the lost profit, could be mitigated.

References

[1] International Energy Agency, "Global EV Outlook 2019," Technical Report, 2019.
[2] I. Pavić, T. Capuder, and I. Kuzle, "Low carbon technologies as providers of operational flexibility in future power systems," Appl. Energy, vol. 168, pp. 724–738, Apr. 2016.
[3] International Renewable Energy Agency, Innovation landscape brief: Electric-vehicle smart charging, Technical Report, 2019.
[4] G. Pasaoglu, D. Fiorello, A. Martino, G. Scarcella, A. Alemanno, A. Zubaryeva, an C. Thiel, "Driving and parking patterns of European car drivers - a mobility survey," European Commission Report, 2012.
[5] ENTSO-E, "ENTSO-E Balancing Report," 2020.
[6] ENTSO-E, "Supporting Document for the Network Code on Load-Frequency Control and Reserves," 2013.
[7] ENTSO-e, "PICASSO MARI," Stakeholder Workshop. 2020.
[8] J. Figgener *et al.*, "The development of stationary battery storage systems in Germany — A market review," *J. Energy Storage*, vol. 29, p. 101153, Jun. 2020.
[9] Ramboll, "Ancillary Services From New Technologies," Technical Report, 2019.
[10] J. Engels, "Integration of Flexibility from Battery Storage in the Electricity Market," PhD Thesis, 2020.
[11] ACER, "ACER Market Monitoring Report 2019 – Electricity Wholesale Markets Volume," ACER Market Monitoring Report 2018 — Electricity Wholesale Markets Volume, 2019.
[12] I. Pavić, Y. Dvorkin, and H. Pandžić, "Energy and reserve co-optimisation - Reserve availability, lost opportunity and uplift compensation cost," IET Gener. Transm. Distrib., vol. 13, no. 2, 2019.
[13] APG, "AFRR-Cooperation Austria/Germany," 2021. [Online]. Available: www.apg.at/en/markt/netzregelung/sekundaerregelung/Kooperation. [Accessed: 24-May-2021].
[14] Z. Zhou, T. Levin, and G. Conzelmann, "Survey of U . S . Ancillary Services Markets," Chicago, 2016.
[15] J. Undrill, "Primary Frequency Response and Control of Power System Frequency," Energy Anal. Environ. Impacts Div. Lawrence Berkeley Natl. Lab., no. February, 2018.
[16] T. Lee, "A Market for Primary Frequency Response?," 2018.
[17] NYISO, Guide 01 Market Participants User's Guide. 2018.
[18] M. Alipour *et al.*, "Stochastic scheduling of aggregators of plug-in electric vehicles for participation in energy and ancillary service markets," *Energy*, vol. 118, pp. 1168—1179, Jan. 2017.

[19] M. Shafie-Khah, M. P. Moghaddam, M. K. Sheikh-El-Eslami, and J. P. S. Catalao, "Optimised performance of a plug-in electric vehicle aggregator in energy and reserve markets," *Energy Convers. Manag.*, vol. 97, pp. 393—408, Jun. 2015.

[20] I. Momber *et al.*, "Risk averse scheduling by a PEV aggregator under uncertainty," *IEEE Trans. Power Syst.*, vol. 30, no. 2, pp. 882—891, Mar. 2015.

[21] S. I. Vagropoulos and A. G. Bakirtzis, "Optimal bidding strategy for electric vehicle aggregators in electricity markets," *IEEE Trans. Power Syst.*, vol. 28, no. 4, pp. 4031—4041, 2013.

[22] P. Sanchez-Martin, S. Lumbreras, and A. Alberdi-Alen, "Stochastic programming applied to ev charging points for energy and reserve service markets," *IEEE Trans. Power Syst.*, vol. 31, no. 1, pp. 198–205, Jan. 2016.

[23] R. J. Bessa and M. A. Matos, "Optimization models for EV aggregator participation in a manual reserve market," *IEEE Trans. Power Syst.*, vol. 28, no. 3, pp. 3085–3095, 2013.

[24] C. Goebel and H. A. Jacobsen, "Aggregator-Controlled EV Charging in Pay-as-Bid Reserve Markets with Strict Delivery Constraints," *IEEE Trans. Power Syst.*, vol. 31, no. 6, pp. 4447—4461, Nov. 2016.

[25] P. Hasanpor Divshali and C. Evens, "Optimum Operation of Battery Storage System in Frequency Containment Reserves Markets," *IEEE Trans. Smart Grid*, vol. 11, no. 6, pp. 4906—4915, Nov. 2020.

[26] M. Merten *et al.*, "Bidding strategy for battery storage systems in the secondary control reserve market," *Appl. Energy*, vol. 268, p. 114951, 2020.

[27] K. Pandžić, I. Pavić, I. Andročec, and H. Pandžić, "Optimal Battery Storage Participation in European Energy and Reserves Markets," *Energies*, 2020.

[28] G. Liu, Y. Xu, and K. Tomsovic, "Bidding strategy for microgrid in day-ahead market based on hybrid stochastic/robust optimization," *IEEE Trans. Smart Grid*, vol. 7, no. 1, pp. 227—237, Jan. 2016.

[29] M. Kazemi *et al.*, "Operation Scheduling of Battery Storage Systems in Joint Energy and Ancillary Services Markets," *IEEE Trans. Sust. Energy*, vol. 8, no. 4, pp. 1726–1735, Oct. 2017.

[30] M. R. Sarker, Y. Dvorkin, and M. A. Ortega-Vazquez, "Optimal participation of an electric vehicle aggregator in day-ahead energy and reserve markets," *IEEE Trans. Power Syst.*, vol. 31, no. 5, pp. 3506–3515, Sept. 2016.

[31] I. Pavić, H. Pandžić, T. Capuder, "Electric Vehicles as Frequency Containment Reserve Providers," in *Proceedings of IEEE International Energy Conference (ENERGYCON)*, Gammarth, Tunisia, Oct. 2020.

[32] B. Han *et al.*, "Day-ahead electric vehicle aggregator bidding strategy using stochastic programming in an uncertain reserve market," *IET Gener. Transm. Distrib.*, vol. 13, no. 12, pp. 2517–2525, Jun. 2019.

[33] M. A. Ortega-Vazquez, "Optimal scheduling of electric vehicle charging and vehicle-to-grid services at household level including battery degradation and price uncertainty," *IET Gener. Transm. Distrib.*, vol. 8, no. 6, pp. 1007-–1016, June 2014.

[34] I. Pavić, H. Pandžić, and T. Capuder, "Electric vehicle based smart e-mobility system – Definition and comparison to the existing concept," Appl. Energy, vol. 272, p. 115153, Aug. 2020.

[35] RTE, "RTE Customer's area - Volumes and prices." [Online]. Available: https://www.services-rte.com/en/view-data-published-by-rte.html [Accessed: 22-Jan-2019].

[36] C. Thiel, A. Alemanno, G. Scarcella, A. Zubareyeva, and G. Pasaoglu, "Attitude of European car drivers towards electric vehicles: a survey," JRC Report, 2012.

[37] G. Pasaoglu *et al.*, "Projections for EV Load Profiles in Europe Based on Travel Survey Data Contact information," JRC Report, 2013.

[38] J. M. Morales *et al.*, Integrating Renewables in Electricity Markets, vol. 205. Boston, MA: Springer US, 2014.